[5]J. O. Linde, Ann. Physik 15, 219 (1932); G. Borelius, Metallwirtschaft 12, 173 (1933); E. Grüneisen, Ann. Phys. (Leipzig) 16, 530 (1933); G. J. van den Berg, *De Electrische Weerstand Van Zuivere Metalen Bij Lage En Zeer Lage Temperaturen* (Amsterdam, 1938); A. N. Gerritsen and J. O. Linde, Physica 18, 877 (1952); E. I. Salkovitz, A. I. Schindler, and E. W. Kammer, Phys. Rev. 98, 543 (1955); 105, 887 (1953); 107, 1549 (1957); D. K. C. MacDonald and W. B. Pearson, Acta Met. 3, 392 (1955); A. T. Robinson and J. E. Dorn, J. Metals Trans. Met. Soc. AIME 3, 457 (1951); P. Alley and B. Serin, Phys. Rev. 116, 334 (1959); C. A. Domenicali and E. L. Christenson, J. Appl. Phys. 32, 2450 (1961); F. T. Hedgecock and W. B. Muir, Phys. Rev. 136, 561 (1964); J. S. Dugdale and Z. S. Basinski, *ibid.* 157, 552 (1967); J. T. Schriempf, in Proceedings of the Seventh Conference on Thermal Conductivity, 1967 (unpublished); Mme. Dreyfus and F. Gautier (unpublished); A. D. Caplin and C. Rizzuto (unpublished).

[6]J. M. Ziman, *Electrons and Phonons* (Clarendon, Oxford, England, 1960), Chap. 7.

[7]A. D. Caplin and C. Rizzuto, Phys. Rev. Letters 21, 746 (1968).

[8]F. Bloch, Z. Physik 59, 208 (1930); A. H. Wilson, see Ref. 3, Chap. 9.

[9]See Ref. 6.

[10]For example, from the detailed variational calculations of E. H. Sondheimer, Proc. Roy. Soc. (London) A203, 75 (1950).

[11]H. B. Callen and T. A. Welton, Phys. Rev. 83, 34 (1951); R. Kubo, J. Phys. Soc. Japan 12, 570 (1957).

[12]The plus or minus sign here refers to the emission or absorption of a phonon quantum in the scattering event.

[13]The largest "experimental value" of a appears to occur for dilute *Au*Fe [D. K. C. MacDonald, W. B. Pearson, and I. M. Templeton, Proc. Roy. Soc. (London) A266, 161 (1962)], where $a \sim 10$ for T of the order of a few °K. Even here the right-hand side of (2.21) is well satisfied.

[14]See Ref. 6, Chap. 9.

[15]Note that $(1/\Omega)\sum_{\vec{q}} \rightarrow [1/(2\pi)^3]\int d^3q$. There is no factor of 2 as in (3.1) for the $\vec{k}$ sums since $\vec{q}$ denotes the momentum transfer which does not carry a spin subscript.

[16]J. Friedel, Can. J. Phys. 34, 1190 (1956).

[17]J. Korringa and A. N. Gerritsen, Physica 19, 457 (1953).

[18]C. A. Domenicali, Phys. Rev. 117, 984 (1960).

[19]From a practical standpoint, it is convenient to compare resistive increments, such as Δ_1 and Δ_2, with the $(T=0)$ residual resistivity.

[20]For example, M. D. Daybell and W. A. Steyert, Phys. Rev. 167, 540 (1968).

[21]E. Grüneisen, Ann. Phys. (Leipzig) 16, 530 (1932); A. N. Gerritsen and J. O. Linde, Physica 18, 877 (1952); W. B. Pearson, Phil. Mag. 46, 911 (1955) (footnote, p. 915); C. A. Domenicali and E. L. Christenson, J. Appl. Phys. 32, 2450 (1961). This effect may also be seen in the recent data of Ref. 20.

[22]See, in particular, A. N. Gerritsen and J. O. Linde, Ref. 5.; C. A. Domenicali and E. L. Christenson, Ref. 5.

[23]a_0 is large but satisfies the inequality (2.19).

[24]For the case of scattering from magnetic impurities, a fully explicit expression for $\tau_0(\epsilon; c, T)$ has been derived; for example, by Y. Nagaoka, Progr. Theoret. Phys. (Kyoto) 39, 533 (1968), and discussed recently by K. Maki, *ibid.* 41, 586 (1969).

[25]A. D. Caplin and C. Rizzuto, Phys. Rev. Letters 21, 746 (1968).

[26]G. Boato and J. Vig, Solid State Commun. 5, 649 (1967).

PHYSICAL REVIEW B VOLUME 2, NUMBER 10 15 NOVEMBER 1970

Anisotropy of the Temperature-Dependent Resistivity of Tin between 8 and 300 °K*

S. K. Case and J. E. Gueths

Physics and Astronomy Department, Wisconsin State University, Oshkosh, Wisconsin 54901

(Received 4 June 1970)

Electrical-resistivity measurements have been performed on five single crystals of pure tin in the temperature interval 8–300 °K. From these measurements, the temperature-dependent anisotropy $(a=\rho_{\parallel}/\rho_{\perp})$ of the electrical resistivity has been determined. A striking maximum in the a-versus-T curve is noted at $T\approx 20$ °K. The features of this curve at high, intermediate, and low temperatures are interpreted in terms of a simplified model for an anisotropic metal. The model predicts that the a-versus-T curve for all electrically anisotropic metals with anisotropy a_∞ as $T\rightarrow\infty$ will exhibit a maximum $a_{\max}=a_\infty^2$ at intermediate or low temperatures.

INTRODUCTION

This paper reports the results of an experimental investigation of the temperature-dependent electrical-resistivity anisotropy of pure tin. Five oriented pure-tin single crystals (less than 3-ppm impurity) were measured between 8 and 300 °K. The anisotropy was determined to be a strongly varying function of temperature for tin. A greatly simplified model for an anisotropic metal is employed to explain the gross features of the a-versus-T data.

The orientation dependence of the resistivity of a tetragonal crystal such as tin may be written in the form

$$\rho(\theta) = \rho_\perp [1 + (a-1)\cos^2\theta], \quad (1)$$

where θ is the angle between the tetrad axis and the current direction, $\rho_\perp$ is $\rho(90°)$, and a, which we

call the anisotropy, is the ratio $\rho(0°)/\rho(90°)$ or alternately $\rho_{\parallel}/\rho_{\perp}$. References to the anisotropic resistivity of noncubic metals are frequently found in the literature,[1-6] usually as asides to research directed at other physical properties. The dependence of the anisotropy of the residual resistivity on impurity type was first explored by Burckbuchler and Reynolds,[7] but the temperature dependence of the anisotropy of the ideal resistivity has not yet been the subject of an experimental investigation. Our objectives in this work were to (i) measure $a(T)$ for an anisotropic metal over an extended temperature range, (ii) attempt an explanation of the features of the anisotropy data and identify the elements of the theory particularly important to considerations of the anisotropy, and (iii) extend, if possible, our model toward generalizing the temperature dependence of $a(T)$ for all anisotropic metals.

EXPERIMENTAL DETAILS

The techniques of sample preparation and orientation are nearly identical to those described by Gueths *et al.*[1] and will not be repeated here. The angles between the tin symmetry axis and the crystal axes for the five crystals studied in this work were 69.6°, 62.2°, 52.0°, 41.7°, and 4.4°. Each sample was a single crystal cylinder with a diameter of approximately 3 mm and a length of approximately 10 cm. Current leads were attached to the ends of the sample by soldering (at one end) and a mechanical contact (at the other). Steel knife-edge contacts separated by a distance of approximately 6 cm served as potential contacts.

The five crystals studied in this work were mounted symmetrically on a sample holder shown schematically in Fig. 1. The holder was positioned at the bottom of a 2-liter nested helium Dewar, and low temperatures were attained by boiling liquid helium (or nitrogen) and transferring the cold He (N_2) gas through a nitrogen-jacketed helium transfer line. The arrangement of Dewars, transfer lines, and controlling electronics was similar to that described by Fleury and Loudon.[8]

Temperature control was achieved by sending a constant current through a calibrated germanium resistance thermometer and monitoring the voltage drop across the resistor with a Leeds and Northrup K-4 potentiometer. The potentiometer was set at the voltage corresponding to the desired temperature, and the off-balance signal (after amplification) was fed into a differential amplifier controlling the heater at the end of the transfer line shown in Fig. 1. At higher temperatures ($T > 25$ °K) the procedure was identical except that a calibrated platinum resistance thermometer (shown in Fig. 1) was employed.

Voltage drops across the crystals were measured

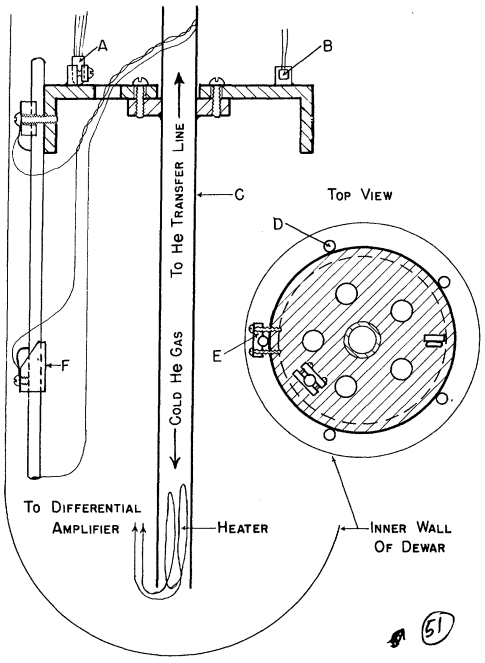

FIG. 1. Specimen holder. Germanium resistance thermometer (A) or platinum resistance thermometer (B) used for temperature control. Cold He gas passes through stainless-steel transfer line (C) past heater and into Dewar. Five cylindrical crystals (D) are anchored thermally and electrically to copper specimen holder by specimen mounts (E). Spring steel voltage probes are secured by upper specimen mounts and by Teflon probe mounts (F).

with a Honeywell 2779 μV potentiometer and a Honeywell 3990 guarded μV null detector. System resolution was approximately 10^{-8} V.

The data were analyzed for indications of temperature gradients down the lengths of the samples or azimuthal gradients about the Dewar symmetry axis. Significant longitudinal gradients would manifest themselves as vertical shifts in all five ρ-versus-T curves with respect to existing ρ-versus-T data for tin. Azimuthal gradients would leave some samples warmer than others. This would result in systematic deviations from linearity in the ρ-versus-$\cos^2\theta$ data at various temperatures, as we assumed that all samples were at the thermometer temperature. Evidence for longitudinal gradients was not found in the data, and although systematic deviations in the ρ-versus-$\cos^2\theta$ data were noted, they were extremely small and well within the uncertainty in the geometrical factors ($\approx 1\%$) of the five crystals.

EXPERIMENTAL RESULTS

The anisotropy of the electrical resistivity of the tin crystals as a function of temperature is shown in Fig. 2. Data determined in several previous

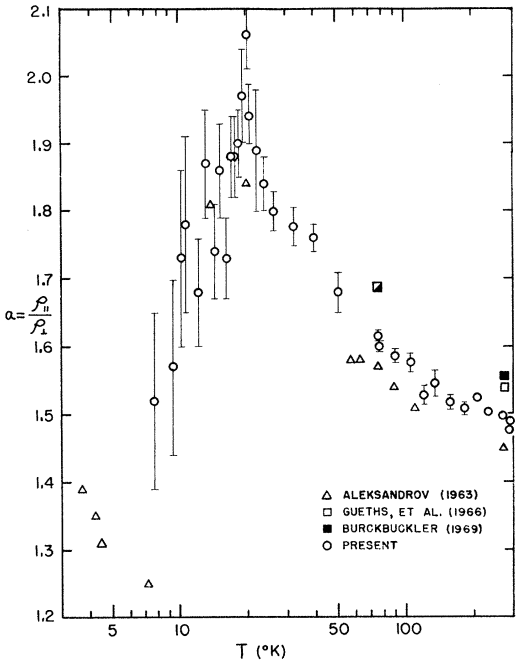

FIG. 2. Anisotropy of electrical resistivity for pure tin as a function of temperature.

studies are included for comparison. Particularly noteworthy features of the curve are the initial slow rise in a as the temperature is decreased below room temperature, the strikingly large variation of a with T, and the maximum in a at $T \approx 20\,^{\circ}\mathrm{K}$.

We will be interested in a_{∞}, the anisotropy as $T \to \infty$, in the analysis of the data. To this end, we plot a versus T^{-2} for $T > 100\,^{\circ}\mathrm{K}$ (Fig. 3). The high-temperature limit for a is found to be approximately 1.48. It should be noted that the exact power dependence for a in this plot is not critical. Approximately the same result would be obtained if we plotted a versus T^{-3}.

The amount by which a rises above its high-temperature limit $(a - a_{\infty})$ is plotted on a logarithmic scale in Fig. 4. Of particular note is the apparent T^{-2} variation of this quantity for $T > 100\,^{\circ}\mathrm{K}$. This vindicates our procedure used to obtain a_{∞} in Fig. 3. The rather extended region of constant a in the vicinity of $T \approx 20\,^{\circ}\mathrm{K}$ is also distinctive. There is some evidence of structure in this curve between 18 and 40 °K, but the size of the error in a precludes a definite statement to this effect.

As T decreases below 15 °K, the error in our anisotropy determinations becomes increasingly larger due to the very low voltages involved in the resistivity determinations (typically less than 10^{-7} V). The evidence, for what it is worth, is that a falls off toward the high-temperature limit (a_{∞}) as $T \to 0$. While the data of Aleksandrov and D'Yakov[2] in Fig. 2 would indicate that a minimum in a is reached in the vicinity of 7 °K, one must be reluctant to draw this conclusion in light of the absence of an error analysis in their work.

Not shown are the ρ-versus-T curves for the five crystals measured in this work. The data were compared to the recent compilation of the National Bureau of Standards[9] and found to be in excellent agreement with previous investigations over the whole temperature range investigated.

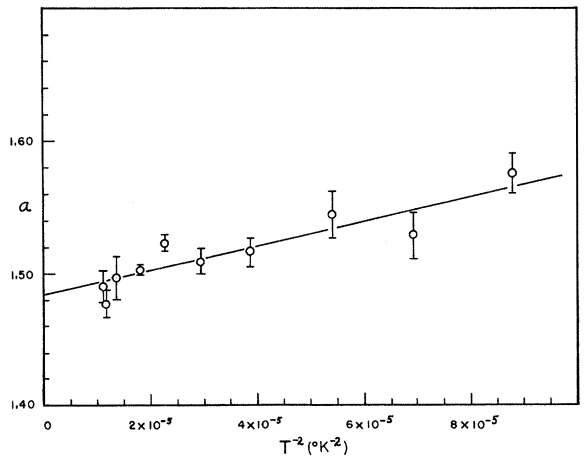

FIG. 3. Determination of a_{∞}, the anisotropy of the electrical resistivity as $T \to \infty$.

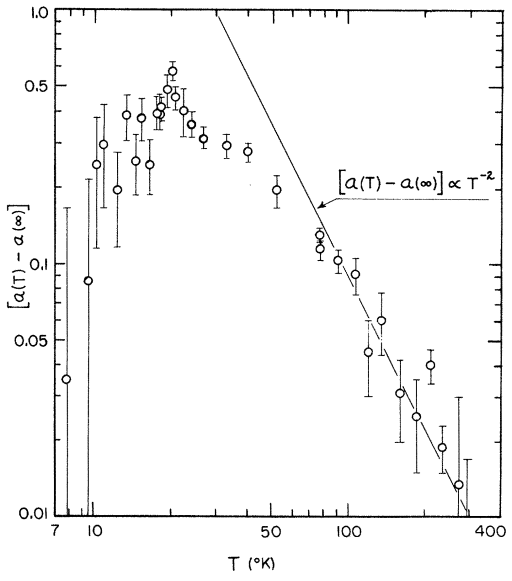

FIG. 4. Temperature-dependent contribution to anisotropy $(a - a_{\infty})$ showing T^{-2} dependence for $T > 100\,^{\circ}\mathrm{K}$ and maximum value at $T \approx 20\,^{\circ}\mathrm{K}$.

DISCUSSION OF RESULTS

The temperature-dependent variation of a for pure tin can be substantially understood in terms of a simplified nearly-free-electron model for an anisotropic metal. We begin with the model proposed by Klemens *et al.*[10] in which the Fermi surface of tin is taken as a sphere in extended momentum space, except in the vicinity of Brillouin-zone boundaries having nonvanishing structure factor. Reasonably large areas of the Fermi surface extend beyond Brillouin-zone boundaries in directions centered about 0°, 60°, and 90° with respect to the c axis and can be expected to contribute significantly to the conduction process. Since the larger areas of the Fermi surface in this model are oriented in such a way that conduction in any direction perpendicular to the c axis is preferred, a is expected to be greater than 1. This agrees with our experimental measurements at all temperatures.

It is convenient to replace this model of the Fermi surface of tin with an even simpler one retaining the features necessary to explain an anisotropic electrical resistivity. Consider a distorted Fermi sphere (or ellipsoid) intersecting a Brillouin-zone structure in the form of a rectangular parallelpiped [Fig. 5(a)]. This structure contains many of the features that are required for tin, having fourfold symmetry about the c axis, an anisotropic Brillouin-zone structure (in the correct sense for tin having $c/a < 1$ in real space), and large areas of the Fermi surface extending beyond the zone boundaries in directions parallel and perperdicular to the symmetry axis.

The fourfold symmetry of the model allows us a further simplification. For the purposes of electrical-conductivity calculations, nothing is lost by considering the tin electron structure in terms of a two-dimensional rectangular Brillouin zone with regions of the Fermi surface extending beyond it directed parallel and perpendicular to the symmetry axis [Fig. 5(b)].

We assume that the only area of the Fermi surface contributing to $\sigma_{\parallel}$, the conductivity parallel to the c axis, is $A_{\parallel}$. Since $\sigma_{\parallel} = (e^2/m)\, n_{\parallel} \tau_{\parallel}$, where $n_{\parallel}$ is the number of electrons available for electrical conduction in the parallel direction, we can write

$$\sigma_{\parallel} \propto A_{\parallel} \tau_{\parallel} , \tag{2}$$

where $\tau_{\parallel}$ is the relaxation time appropriate to the resistive processes present. Using a similar argument, we find that $\sigma_{\perp} \propto A_{\perp} \tau_{\perp}$, so that

$$a = \rho_{\parallel}/\rho_{\perp} = \sigma_{\perp}/\sigma_{\parallel} = (A_{\perp}/A_{\parallel})(\tau_{\perp}/\tau_{\parallel}) . \tag{3}$$

In order to make our simplified model as realistic as possible, we have contrived the situation so that both zone boundaries slicing the Fermi surface into segments having areas $A_{\parallel}$ and $A_{\perp}$ are oriented such that U processes involving them are effective resistive mechanisms. In other words, the significant zone boundaries are perperndicular to the applied electric field when considering $\rho_{\parallel}$ and $\rho_{\perp}$. This is necessary since U processes are the only significant resistive processes over much of the temperature range covered in this work.

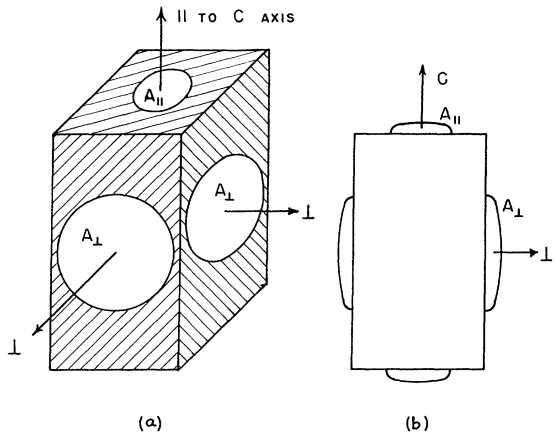

FIG. 5. (a) Simplified model of Fermi surface extending beyond Brillouin-zone boundaries showing areas available for conduction in the parallel and perpendicular directions. Fourfold symmetry about c axis allows further simplication to a two-dimensional model (b).

At temperatures between 10 °K and several hundred °K, the ideal resistivity of these specimens exceeds by far the residual resistivity. At the same time, the momentum transfer $\delta\vec{K}$ associated with a typical electron-phonon interaction is small compared with the distance between a typical conduction-electron state and the intersection between the Fermi surface and the Brillouin-zone boundary. Therefore, the electron state does a random walk on the large Fermi-surface areas in this temperature region. The relaxation time appropriate for inclusion in Eq. (3) takes the form

$$\tau = \tau_0 + \tau_{RW} , \tag{4}$$

where τ_0 is the relaxation time characteristic of the electron-phonon scattering process and τ_{RW} is the mean time required for an electron state on the Fermi-surface segment to move via random walk to a point within $|\delta\vec{K}|$ of the Brillouin-zone boundary. Once the state arrives near the zone boundary, a single scattering event can take it to the boundary where it undergoes a U process and is scattered resistively.

Consider first the form of τ_{RW}. An electron state having suffered m small-angle phonon-scattering events has moved a distance $|\sum\delta\vec{K}| = \sqrt{m} \times |\delta\vec{K}|$, where $|\sum\delta\vec{K}|$ is the most probable total distance moved on the Fermi surface. τ_{RW} is equal

to $m\tau_0$, so that

$$\tau = \tau_0 + m\tau_0 = \tau_0 + (|\sum \delta\vec{K}|^2/|\delta\vec{K}|^2)\,\tau_0 \ . \tag{5}$$

We note that $|\delta\vec{K}| \propto T$ (for small-angle scattering) and $|\sum\delta\vec{K}|^2 \propto A$ when the electron state is brought to the boundary, so that τ in Eq. (3) takes the form

$$\tau = \tau_0 + CA/T^2 \ , \tag{6}$$

where C is a constant within which we deposit our ignorance of a variety of proportionality constants. In the following, we will assume that τ_0 is isotropic and that $C_\parallel = C_\perp$.

High Temperatures

As $T \to \infty$, the electron-phonon interactions produce $\delta\vec{K}$'s large enough to consistently bring the electron state to the zone boundary. Therefore, $\tau_{RW} \to 0$ for both parallel and perpendicular directions, and Eq. (3) yields

$$a_\infty = A_\perp/A_\parallel \ , \tag{7}$$

since $\tau_\perp = \tau_\parallel = \tau_0$. For tin, we find that $a_\infty = 1.48$ from the extrapolation in Fig. 3.

Intermediate Temperatures

As the temperature decreases, $|\delta\vec{K}|$ decreases, and electron states will first begin to undergo random walk on the largest portions of the Fermi surface (the portions directed perpendicular to the c axis). In this temperature region, we expect that $\tau_\parallel = \tau_0$, and $\tau_\perp = \tau_0 + CA_\perp/T^2$, so that, combining Eqs. (3), (6), and (7), we obtain

$$a = (a_\infty/\tau_0)\,(\tau_0 + CA_\perp/T^2) = D/T^2 + a_\infty \ . \tag{8}$$

Rearranging terms, we obtain $a - a_\infty = D/T^2$. The T^{-2} dependence of $(a - a_\infty)$ is noted in Fig. 4.

Low Temperatures

At lower temperatures, $|\delta\vec{K}|$ decreases until electron states on both areas of the Fermi surface undergo random walk before suffering a resistive U process. Eventually, the random-walk component of the relaxation time dominates both $\tau_\perp$ and $\tau_\parallel$, and Eq. (3) becomes

$$a = a_\infty\,\tau_\perp/\tau_\parallel = a_\infty^2 \ . \tag{9}$$

Equation (9) predicts that the maximum in the a-versus-T curve should be broad over the region in which the foregoing assumptions are satisfied and should be equal to a_∞^2. From Fig. 2, $a_{max} \approx 2.0$, while $a_\infty^2 \approx 2.2$. The numerical agreement is sufficient to be encouraging, when one considers the degree of approximation involved in this model.

Lowest Temperatures

According to the preceding arguments, we would expect that as $T \to 0\,^\circ$K in an ideal metal crystal, $a_0 = a_\infty^2$. However, ideal crystals are not available to the laboratory, and as the temperature is lowered further, significant contributions to the resistivities ($\rho_\parallel$ and $\rho_\perp$) due to imperfection scattering (typically large angle) begin to emerge. Thus, the relaxation-time advantage that the electron states have on the larger segments of the Fermi surface is increasingly eroded as the temperature is decreased. If one assumes that Matthiessen's rule holds on each Fermi-surface segment and that the relaxation time for imperfection scattering is isotropic, one can easily show that a is of the form

$$a = a_\infty\left(\frac{\rho_{i\parallel}/\rho_{0\parallel} + 1}{\rho_{i\perp}/\rho_{0\perp} + 1}\right), \tag{10}$$

where ρ_i and ρ_o are the ideal and residual electrical resistivities, respectively. For our samples, we find that $\rho_{0\parallel} \approx 3\times10^{-9}\ \Omega$cm and $\rho_{0\perp} \approx 2\times10^{-9}\ \Omega$cm from an examination of the ρ-versus-T curves in the temperature interval 7–12 °K. Using Eq. (10), we conclude that a significant drop in a due to residual resistivity contributions should not occur until $T < 10\,^\circ$K. This is consistent with the features of Fig. 4 that can be seen above the rising scatter in the data.

In a sense, it is uncanny that this model which ignores (i) the anisotropy of the phonon spectrum, (ii) the anisotropy of the electron-phonon interaction, (iii) any real detail of the Fermi surface of tin, and (iv) the anisotropy of the impurity resistivity is so successful in explaining the features of our data. On the other hand, the dominant role that U processes play in the resistive processes is reasonably well accounted for in our model. The degree to which this model of an anisotropic metal is useful as a general one can only be tested with data on other pure-metal crystals.

SUMMARY

The temperature dependence of the electrical-resistivity anisotropy has been measured for pure tin in the temperature interval 8–300 °K. An extremely simplified model of an anisotropic metal is quite successful in explaining the gross features of the data. Extrapolation of this model to other anisotropic metals suggests that the features of the anisotropy-versus-temperature curves for all pure noncubic metals should be similar, having a maximum anisotropy approximately equal to the square of a_∞, the anisotropy as $T \to \infty$. The lack of data on other anisotropic metals precludes us from checking this point at this time.

ACKNOWLEDGMENTS

The authors wish to thank Dr. P. G. Klemens and Dr. D. Ginsberg for several extremely helpful communications relating to the relaxation time of an electron state on a Fermi-surface segment. We also wish to thank J. Perry for his technical assistance.

*Supported by the Research Corporation and the Wisconsin State University Board of Regents Research Fund. Part of this work was performed with support of the Undergraduate Research Participation program of the National Science Foundation, under Grant No. GY-5716.

[1]J. E. Gueths, C. A. Reynolds, and M. A. Mitchell, Phys. Rev. 150, 346 (1966).

[2]B. N. Aleksandrov and I. G. D'Yakov, Zh. Eksperim. i Teor. Fiz. 43, 852 (1962) [Soviet Phys. JETP 16, 603 (1963)].

[3]V. B. Zernov and Yu. V. Sharvin, Zh. Eksperim. i Teor. Fiz. 36, 1038 (1959) [Soviet Phys. JETP 9, 737 (1959)].

[4]P. W. Bridgman, Proc. Am. Acad. Arts Sci. 68, 95 (1933); 60, 305 (1925).

[5]B. Chalmers and R. H. Humphrey, Phil. Mag. 25, 1108 (1938).

[6]E. Grüneisen and E. Goens, Z. Physik 26, 250 (1924).

[7]F. V. Burckbuchler and C. A. Reynolds, Phys. Rev. 175, 550 (1968).

[8]P. A. Fleury and R. Loudon, Phys. Rev. 166, 514 (1968).

[9]L. A. Hall, NBS Technical Note 365, 1968 (unpublished).

[10]P. G. Klemens, C. Van Baarle, and F. W. Gorter, Physica 30, 1470 (1964).

PHYSICAL REVIEW B VOLUME 2, NUMBER 10 15 NOVEMBER 1970

Lattice-Dynamical Theory of the Diffusion Process. I. Isotope Effect in Cubic Metals†

B. N. Narahari Achar

Argonne National Laboratory, Argonne, Illinois 60439

(Received 18 June 1970)

A lattice-dynamical theory of diffusion based on the fluctuations in a certain reaction coordinate first used by Flynn is presented. The theory of vibrations of isotopic impurities in a crystal is applied to evaluate the parameter ΔK that describes the isotope effect in diffusion. Numerical results for Cu, Ag, Au, Al, Ni, Co, Pb, Na, and α-Fe are presented. The effect of both relaxation near the vacancy and temperature on ΔK are also studied.

I. INTRODUCTION

Recently, there has been renewed interest in the study of diffusion phenomena in metals, and the state of the art has been described by Peterson.[1] The degree of accuracy and sophistication that has been achieved experimentally, with the advent of tracer techniques, is paralleled by some significant theoretical developments. Glyde,[2] while examining the theories of rate processes in solids, showed that the dynamical approach used by Rice, and Rice and Frisch[3] is equivalent in formal content to the equilibrium statistical-mechanical approach used by Vineyard.[4] Franklin[5] formulated an anharmonic theory of atomic migration that resembles the equilibrium statistical-mechanical approach. Flynn[6] presented a dynamical theory of diffusion in the elastic continuum limit. His theory, based on fluctuations in a specific reaction coordinate, has met with considerable success in accounting for the diverse features of atomic migration. Impressive as these efforts are, quantitative calculation of specific parameters that appear in the theory of diffusion have been largely unsatisfactory. One example is ΔK, which, together with a correlation factor f, is a measure of the isotope effect in diffusion. Although accurate experimental measurements of the dependence of tracer diffusion rate on isotopic mass have been available for quite some time,[1] theoretical calculations of ΔK with a comparable degree of sophistication have not been available. In a recent paper, Glyde[7] rederived the expression for the classical jump rate Γ for tracer diffusion to demonstrate clearly its mass dependence; however, no numerical application to real systems was made. Huntington *et al.*[8] have attempted to calculate several fundamental parameters involved in the diffusion phenomena by computer simulation of atomic migration. They evaluated the parameter ΔK on the basis of the reaction rate theory, where ΔK is equal to the ratio of the kinetic energy of the moving atom, in the dissolu-